

# Predictive biomarkers and metabolic hallmark of postoperative hypoxaemia

Raluca Georgiana Maltesen<sup>1,2</sup> · Munsoor Ali Hanifa<sup>1</sup> · Sergey Kucheryavskiy<sup>3</sup> · Shona Pedersen<sup>4</sup> · Søren Risom Kristensen<sup>4</sup> · Bodil Steen Rasmussen<sup>2,5</sup> · Reinhard Wimmer<sup>1</sup> 

Received: 9 November 2015 / Accepted: 18 February 2016 / Published online: 18 March 2016  
© Springer Science+Business Media New York 2016

## Abstract

**Introduction** Pulmonary dysfunctions resulting in postoperative hypoxaemia is a common complication of cardiac surgery. The disease is challenging as it lacks predictive biomarkers. Since a comprehensive metabolic overview of lung microvasculature injury is lacking, we have compared the metabolome of patients undergoing cardiac surgery from blood collected on the first postoperative day from the pulmonary artery and left atrium.

**Objectives** To identify predictive biomarkers and metabolic hallmark of pulmonary hypoxaemia.

**Methods** Blood samples collected on the first postoperative morning from 47 patients were analysed by nuclear magnetic resonance and multivariate statistics. Patients' metabolomes were correlated to the level of partial

pressure of arterial oxygen (PaO<sub>2</sub>) without supplementary oxygen treatment measured on the third postoperative day. **Results** Three days postoperatively, 32 patients suffered from hypoxaemia. Spectra recorded on samples collected on the first morning postoperatively revealed metabolic perturbations causing disease progressing. Regression modelling found a 0.97 association between metabolome and PaO<sub>2</sub>. Classification modelling distinguished patients according to later hypoxaemia. Sixty-four metabolites were identified as the early hallmarks of disease, of which several showed significant correlations with PaO<sub>2</sub> ( $r > 0.55$ ,  $p \leq 0.00001$ ). The tricarboxylic acid cycle, amino acid and lipid metabolism, together with redox homeostasis were all found affected. An integrated overview reveals complex cross-talk between pathways that can be related to the pathogenesis of hypoxaemia: damaged alveolar-capillary barrier, edema formation, peroxidation, oxidative stress, impaired antioxidant defense, and cell damage.

**Conclusion** Our results indicate unique phenotypes triggering progression into pulmonary dysfunction resulting in postoperative hypoxaemia. The metabolic hallmarks identified offer important targets for future treatments.

**Electronic supplementary material** The online version of this article (doi:10.1007/s11306-016-1018-5) contains supplementary material, which is available to authorized users.

✉ Reinhard Wimmer  
rw@bio.aau.dk

<sup>1</sup> Department of Chemistry and Bioscience, The Faculty of Engineering and Science, Aalborg University, Frederik Bajers vej 7H, 9220 Aalborg, Denmark

<sup>2</sup> Department of Clinical Medicine, The Faculty of Medicine, Aalborg University, Aalborg, Denmark

<sup>3</sup> Department of Chemistry and Bioscience, The Faculty of Engineering and Science, Aalborg University, Niels Bohrsvej 8, 6700 Esbjerg, Denmark

<sup>4</sup> Department of Clinical Medicine, Clinical Biochemistry, The Faculty of Medicine, Aalborg University Hospital, Aalborg, Denmark

<sup>5</sup> Department of Clinical Medicine, Anaesthesia and Intensive Care, The Faculty of Medicine, Aalborg University Hospital, Aalborg, Denmark

**Keywords** Cardiac surgery · Pulmonary dysfunction · Hypoxaemia · Metabolome · Pathways · NMR

## 1 Introduction

Pulmonary dysfunction remains to be the most common complication to cardiac surgery (Clark 2006; Ng et al. 2002). Disturbance of the alveolar-endothelial barrier affects the pulmonary gas exchange (Ng et al. 2002; Singh et al. 1992) with development of postoperative hypoxaemia with nadir values of partial pressure of oxygen in arterial

blood ( $\text{PaO}_2$ ) on the third postoperative day (Ng et al. 2002; Rasmussen et al. 2007).

Disturbance of the alveolar-endothelial barrier is part of the acute lung injury syndrome which is a life-threatening condition (Matthay and Zimmerman 2005; Perl et al. 2011; Ware et al. 2010; Wheeler and Bernard 2007), affecting more than one million individuals worldwide every year (Oeckler and Hubmayr 2008). The injury can develop within a week (Stephens et al. 2013) after direct or indirect pathophysiological events such as sepsis, pneumonia, cardiopulmonary bypass (CPB), and severe trauma (Oeckler and Hubmayr 2008; Perl et al. 2011; Reiss et al. 2012; Stephens et al. 2013; Weissman 2004). Regardless of the initial triggering factor, the final result is abnormal gas exchange (Apostolakis et al. 2009) caused by excessive inflammation (Milot et al. 2001) and disordered coagulation (Reiss et al. 2012; Wheeler and Bernard 2007). Endothelial cell swelling, cellular junction widening, edema accumulation, denuded alveolar membranes, increased pinocytosis, and alveolar collapse are the hallmarks of this dysfunction (Rubinfeld and Herridge 2007).

Currently, no therapeutic intervention has proven useful in impeding disease progression into a state of hypoxaemia which is one of the criteria for acute lung injury. (Fremont et al. 2010; Matthay et al. 2012; Perl et al. 2011) As such, identifying patients at risk of developing clinically important hypoxaemia earlier in the course of their illness would enable the development of therapeutic options targeting the disease (Gajic et al. 2011).

Substantial efforts have been made to understand multiple mechanisms involved in acute lung injury (Bhargava and Wendt 2012; Levitt et al. 2009; Matthay et al. 2012; Ng et al. 2002). In general, the research is focused on understanding the delicate balance between protective and injurious immunologic responses. Although little is known about metabolic activity during the injury, recent studies have reported that the sites of inflammation are characterized by significant metabolic shifts followed by fundamental changes in tissue phenotypes (Kominsky et al. 2010). These changes can be revealed by applying metabolomics (Nicholson et al. 1999, 2002), which screens for metabolite perturbations in a biological system as response to pathophysiological modification (Nicholson et al. 1999). Furthermore, it identifies characteristic disease phenotypes that reflect the connection between tissue histology and environmental, genetic, and immunologic factors (Nicholson et al. 2002). Hence, metabolomics is powerful tool for examining disease-related metabolic changes and in discovering biomarkers (Shlomi et al. 2009).

The metabolic shifts during lung injury have partly been revealed (Evans et al. 2014; Rogers and Matthay 2014; Serkova et al. 2008; Stringer et al. 2011). These changes

are related to energy depletion (Serkova et al. 2008), oxidative stress, apoptosis (Evans et al. 2014), and endothelial disruption (Stringer et al. 2011). No studies have characterized the metabolic phenotypes in patients undergoing coronary artery bypass grafting (CABG) involving ischemia–reperfusion through the use of CPB, a well-established risk factor for developing this condition due to an indirect pathophysiological event (Ng et al. 2002). As pulmonary dysfunction remains the most common complication of cardiac surgery (Clark 2006; Ng et al. 2002), we intend to identify biomarkers and the metabolic hallmarks of postoperative hypoxaemia. Finding and defining perturbations in the metabolome may explain how inflammatory and coagulation mediators orchestrate the metabolism.

We hypothesized that early stages of pulmonary dysfunction following cardiac surgery may be reflected at the metabolite level and precede the development of hypoxaemia on the third postoperative day. We therefore investigated metabolite changes in blood collected from the pulmonary artery (PA) and left atrium (LA) on the first postoperative morning in order to describe changes in the systemic and pulmonary microvasculature. While both samples reflect systemic changes of the metabolome, we expected that metabolic processes confined to the lungs would be reflected in the difference between the LA and PA samples.

## 2 Methods

### 2.1 Patient cohort and diagnosis

Patients scheduled for elective CABG with use of CPB were consecutively included in the study after the informed consent was obtained (study registered at clinicaltrials.gov, NCT02475694). Inclusion criteria were adults above 18 years of age and in treatment with statins. Exclusion criteria were treatment with steroids or other immune suppressor therapies. All patients were monitored with a pulmonary as well as a LA catheter inserted after induction of anesthesia and removed 20 h after weaning from CPB. Of the total cohort of 50 patients, the LA catheter was displaced in three patients at 16 h, giving a cohort of 47 patients in the present study. Information regarding patients enrolled in this study is provided in Table 1 Supplementary.

All patients were spontaneously breathing at all times, but the majority was treated with supplementary oxygen postoperatively to achieve peripheral oxygen saturation ( $\text{SpO}_2$ ) above 95 %. The clinical diagnosis was based on the ratio between partial pressure of oxygen and fraction of inspired oxygen ( $\text{PaO}_2/\text{FiO}_2$ ) calculated from  $\text{PaO}_2$

measured in arterial blood samples collected from the radial artery 72 h after weaning from CPB and in order to standardize the measurements, arterial blood samples were taken while patients were breathing atmospheric air for at least 10 min.

### 2.1.1 Samples preparation

To avoid analytical bias due to sample collection, all blood samples were collected and prepared by the same person. Blood samples were obtained exactly 16 h after weaning from the CPB circuit. This time point was chosen because it lies on the first morning postoperatively, while patients still were fasting. Blood samples were taken simultaneously from the tip of a PA catheter placed after induction of anaesthesia and from a catheter placed by the surgeons in the LA after opening of the pericardium. Subsequently, serum was prepared according to standard procedures, where blood samples were allowed to clot at room temperature for 30 min, followed by centrifugation at 3000 rpm for 10 min. Aliquots of LA and PA serum were immediately stored at  $-80^{\circ}\text{C}$  for 3 years.

### 2.1.2 Biochemical analysis

Blood gas measurements were performed on an ABL837 blood gas analyzer (Radiometer, Copenhagen). Biochemical assays of serum creatinine, albumin, lactate dehydrogenase, and C-reactive protein (CRP) were performed on the multiparametric autoanalyser VITROS FS 5.1 (Ortho Clinical Diagnostics, Raritan, New Jersey, USA) using dedicated reagents. The results are presented in Table 1 Supplementary.

### 2.1.3 Sample preparation for NMR

Prior to NMR measurements, samples were thawed for 2 h at  $4^{\circ}\text{C}$ , vortexed, and centrifuged for 5 min at  $4^{\circ}\text{C}$  and 12,100 g to remove cells and other precipitated materials. Aliquots of 400  $\mu\text{L}$  of supernatant were mixed with 200  $\mu\text{L}$  0.2 M phosphate buffer (pH 7.4, uncorrected meter reading) in  $^2\text{H}_2\text{O}$  (99 %  $^2\text{H}$ ) to minimize variations in pH and to reduce serum viscosity. Throughout the whole process, the samples were kept on ice. The mixture was pipetted into a 5-mm NMR tube and kept at  $5^{\circ}\text{C}$  until NMR acquisition (not longer than 24 h).

**2.1.3.1 NMR measurements** Spectra were acquired on a Bruker DRX-600 NMR spectrometer (Bruker BioSpin, Germany and Switzerland) equipped with a TXI (hydrogen, carbon, nitrogen) probe (Bruker BioSpin, Switzerland) operating at 600.13 MHz for  $^1\text{H}$ . TopSpin 1.3 was used for the acquisition. The experiments were acquired at a

constant temperature of 310.1 K ( $37^{\circ}\text{C}$ ). For the analysis, a  $T_2$  relaxation-edited Carr–Purcell–Meiboom–Gill (CPMG) (Meiboom and Gill 1958) experiment was used. This experiment attenuates broad signals from slowly tumbling proteins and lipoproteins. 128 free induction decays (FIDs) were collected with 32768 complex data points over a spectral width of 11.97 ppm and an acquisition time of 2.28 s. A relaxation delay of 2 s was applied between each FID during which weak continuous wave irradiation ( $\gamma\text{B}_1/2\pi = 26.6\text{ Hz}$ ) was applied at the water frequency (presaturation). The total spin-echo relaxation delay was 67.4 ms and consisted of  $(\tau-\pi-\tau)$  elements, where  $\tau$  is a delay of 0.4 ms and  $\pi$  is a  $180^{\circ}$  pulse of 22  $\mu\text{s}$  length. Spectral processing was carried out in TopSpin version 2.1 (Bruker BioSpin, Germany). Prior to Fourier transformation, exponential multiplication corresponding to a line broadening of 0.3 Hz was applied to the FIDs, which were further zero-filled by a factor of 2 to double the number of points. Spectra were manually phase- and baseline- corrected, and the methyl signal of lactate was used as chemical shift reference at 1.33 ppm.

For metabolite identification, three types of two-dimensional (2D) experiments were acquired. 2D J-resolved  $^1\text{H}$ -NMR experiments, with water pre-saturation during a 2 s relaxation delay were acquired with 8 FIDs for each of the 80 increments. Spectral width was set to 11.6 ppm and 54.7 Hz in F2 and F1 direction, respectively. Prior to 2D-Fourier transformation, both dimensions were multiplied by an unshifted sine bell function and the number of points was doubled by zero-filling. Further, spectra were tilted by  $45^{\circ}$  and symmetrized along the F1 axis. After processing, the skyline projections of 2D J-resolved spectra were manually baseline corrected and calibrated using the center of the methyl signal of lactate. 2D homonuclear  $^1\text{H}, ^1\text{H}$ -TOCSY (Total Correlation Spectroscopy) and  $^1\text{H}, ^{13}\text{C}$ -HSQC (Heteronuclear Single Quantum Coherence) spectra with presaturation were run on representative samples, with different number of FIDs, increments, spectral widths and mixing times in order to focus on different spectral regions. Information obtained from these spectra was used to find matching metabolites in the Human Metabolome Database (Wishart et al. 2007). Further metabolite assignments were performed using AMIX (v. 3.9.10, Bruker BioSpin), BRUKER bbiorecode database (v. 2.7.0–2.7.3), and literature.

**2.1.3.2 Quantification of NMR data** It was performed using the AMIX multi integration tool. Peaks of interest were integrated using the line shape analysis option with a fixed noise factor of 3.5 and a line shape threshold of 0.01. Peaks were integrated using the sum of all points in the region as the integration mode, and normalized to the glucose metabolite region (3.52 ppm (H-5 of  $\beta$ -glucose)

and 5.24 ppm (H-1 of  $\alpha$ -glucose)). A 36:64 equilibrium distribution between  $\alpha$ - and  $\beta$ -glucose was used in the calculations. To calculate the concentration of a given metabolite, we used the following formula:

$$C_X(\text{mM}) = \frac{I_X}{N_X} \cdot C_{\text{Glucose}} \cdot 0.64 \frac{N_{\beta\text{-Glucose}}}{I_{\beta\text{-Glucose}}}$$

where  $C_X$  is metabolite concentration in mM,  $I_X$  is the integral of the metabolite  $^1\text{H}$  peak,  $N_X$  is the number of protons contributing to the metabolite  $^1\text{H}$  peak,  $C_{\text{Glucose}}$  is the chemically determined glucose concentration,  $0.64N_{\beta\text{-Glucose}}$  is the number of protons contributing to the  $\beta$ -glucose signal (at 3.52 ppm) used as reference multiplied by 0.64 (the mole fraction of  $\beta$ -glucose), and  $I_{\beta\text{-Glucose}}$  is the integral of the  $\beta$ -glucose signal at 3.52 ppm.

**2.1.3.3 NMR data preprocessing** CPMG spectra were converted into an n-by-m matrix ( $n = 94$  LA and PA samples from 47 patients,  $m = 8700$  equal buckets of 0.001 ppm width) in AMIX (Analysis of MIXtures software package, version 3.9.10, Bruker BioSpin, Germany) using the region between  $\delta$  9 and 0 ppm, and excluding the water signal region between 4.80 and 4.5 ppm. Further processing and multivariate modelling were carried out in MATLAB R2011b (Mathworks, Natick, MA) coupled with PLS-Toolbox 6.5 (Eigenvector Research, Wenatchee, WA). Binned data was *i*Coshifted (Savorani et al. 2010), normalized to lactate concentration measured 16 h after surgery, log transformed, and autoscaled.

#### 2.1.4 Multivariate modelling

Several mathematical and statistical modeling approaches were employed to relate the preprocessed NMR data to disease phenotypes. Supervised partial least-squares (Wold et al. 1984) (PLS) regression analysis was used to predict the hypoxaemia score values used in diagnosis on the third day postoperatively. PLS discriminant analyses (Wold et al. 1983) (PLS-DA) was applied to evaluate the diagnostic possibilities of NMR and to discover predictive markers. Due to the large number of variables, several variable selection methods (Li et al. 2009; Norgaard et al. 2000; Wold et al. 2001) were employed. Most important variables obtained by each method were combined into a new data matrix, which was used to build a final PLS and PLS-DA model. For each model, a multivariate mathematical equation was obtained which provided scores for each patient derived from the association between intensities and later outcome. The most significant variables were then identified and quantified. The significance of each metabolite was assessed by the variable importance in projection (Eriksson et al. 2001) (VIP) scores. The sign (positive and negative) of loadings were used to determine

which group the corresponding metabolite was a potential marker for.

To establish confidence in our results, we adopted two complementary validation approaches. First, Monte-Carlo cross-validation was applied to reduce the risk of overfitting, by re-sampling the training set (70 % of samples) and cross-validation set (30 % of samples) 5000 times. In each resampling, 14 randomly selected samples were left for prediction, and 33 remaining samples were used to create the model. The omitted samples were then predicted, and a cross-validated (CV) correlation fit (for PLS regression) or classification fit (for PLS-DA) together with a root mean square error of cross-validation (RMSECV) were calculated each time. The final results represent average results of each parameter from the 5000 runs. The average RMSECV was further used to detect the optimal number of latent variables for both PLS and PLS-DA models. This validation procedure gave us an indicator of how well the model might work in predicting future samples (Xia et al. 2013). A second level of model validation was performed by using permutation testing (Good 2011). Here, the models were tested for randomness, to show that no other model performed equally well or better than the main prediction model. After scrambling the group and hypoxaemia score labels 500 times and performing PLS-DA and PLS regression modelling, respectively, we compared the ‘true’ optimal model with the permuted models. The ‘true’ model performance was then statistically compared to the distribution of the permuted models, and a  $p$  value was calculated by means of Wilcoxon’s test. A  $p$  value  $< 0.05$  was considered significant, meaning that the predictive power of our approach was significantly associated with disease phenotypes and hypoxaemia scores, and was not a false-positive association resulting from random prediction.

Additionally, variables found important in the analysis were further used to assess the influence of other potential influencing factors such as gender, age, body mass index, smoking habits, hypertension, and other diseases such as diabetes and chronic lung disease. For each of the potentially influencing factors, we performed a PLS-DA model and assessed its sensitivity, specificity, and accuracy.

As the receiver operating characteristic (ROC) curve analysis is considered to be the standard method for assessing diagnostic tests performance (Obuchowski et al. 2004; Xia et al. 2013), we chose to present all our results using this test. The multivariate ROC curve analysis based on both the calibration and CV set was performed to judge how well PLS-DA models work in predicting new samples. Here, the models’ performances were assessed by considering the frequency with which PLS-DA produced: true positives (the number of sick patients correctly identified), true negatives (the number of unaffected patients correctly



identified), false positives (the number of unaffected patients incorrectly identified as hypoxaemia patients), and false negatives (the number of sick patients incorrectly identified as unaffected). By summarizing these values into the proportion of hypoxaemia patients that were correctly classified as positive and the proportion of unaffected patients that were correctly classified as negative, the models' sensitivities and specificities were assessed:

$$\text{Sensitivity} = \frac{\text{True positives}}{\text{True positives} + \text{False negatives}}$$

$$\text{Specificity} = \frac{\text{True negatives}}{\text{True negatives} + \text{False positives}}$$

### 2.1.5 Statistics

The Statistical Package and Services Solutions software v22.0 was used for the univariate statistical analysis. Descriptive statistics were computed for each group and the quantitative data was summarized using mean, median, and standard deviation. Wherever appropriate, data was visualized by using the Matlab script 'notBoxPlot.m' (Campbell 2010) representing the mean, standard error of mean, standard deviation, and outliers.

The Shapiro–Wilk normality test was applied followed by either parametric or nonparametric methods. When comparing metabolite differences between unaffected and hypoxaemia patients ( $\text{PaO}_2 < 8.4$  kPa), either an independent  $t$  test or Mann–Whitney U test was used. When comparing differences between the three groups (unaffected, mild, severe), either one way analysis of variance (ANOVA) with Tukey HSD or Dunnett T3 (depending on homogeneity of variance) multiple comparison post hoc tests, or the Kruskal–Wallis test with Dunn's post hoc test were applied. When comparing data between the LA and PA, a paired  $t$  test or the nonparametric analogue Wilcoxon-signed rank sum test was used. Significance was set at  $p < 0.05$ .

In order to visualize global changes between groups, the means or medians (depending on data distribution) of each metabolite in the corresponding group were calculated. As such, metabolite fold changes were calculate as the ratio between mild and unaffected and severe and unaffected patients with the formula:

$$FC_{\frac{M(orS)}{U}}(\%) = \frac{M(orS) - U}{U} \cdot 100$$

where FC is fold change in percentage, M is mild, U is unaffected, S is severe.

Because the ratio between two metabolite concentrations may carry more information than the two metabolites alone, the freely available web-based tool ROC Curve

Explorer & Tester (ROCCET) was used to compute all possible pairs of metabolite combinations that could be related to later outcomes. Metabolite ratios exhibiting statistical significance ( $p < 0.05$ ) were further used as biomarker candidates.

The association between metabolites and  $\text{PaO}_2$  values obtained 3 days postoperatively were assessed by Pearson's correlation analysis. ROC curves were established to determine the prognostic value of each biomarker in future diagnosis. The area under the curve (AUC) and corresponding 95 % confidence intervals are provided.

## 3 Results

Hypoxaemia is indicative of the severity of lung injury, being measured by the partial pressures of oxygen in arterial blood ( $\text{PaO}_2$ ) or the ration between  $\text{PaO}_2$  and the fraction of inspired oxygen ( $\text{FiO}_2$ ) (De Backer et al. 1997; Routsis et al. 1999). Two days postoperatively some patients showed signs of hypoxaemia; however, while several patients' blood oxygenation levels return to normal the following day, others worsened. As lung dysfunction is known to develop within 72 h postoperatively, and due to the  $\text{PaO}_2$  changes observed during the second and third postoperative day (Pearson correlation coefficient  $r = 0.49$ ,  $p = 0.0003$ ), the  $\text{PaO}_2$  values measured 72 h postoperative were used as end-points in this study. As such, three days postoperatively, 15 patients showed no signs of hypoxaemia and 32 developed hypoxaemia, of which 9 presented severe hypoxaemia (Supplementary Table 1).

### 3.1 Metabolome screening reveals early signs of disease

The systemic and pulmonary phenotypes were monitored by  $^1\text{H}$  nuclear magnetic resonance (NMR) spectroscopy. A typical one dimensional (1D) serum NMR spectrum is characterized by broad resonances from lipids and glycoproteins, and narrow resonances from glucose, lactate, and citrate, among others. Spectra of two samples collected on the first postoperative day (exactly 16 h after weaning from CPB), one from a patient not developing hypoxaemia ( $\text{PaO}_2 = 10.7$  kPa), and one from a patient developing hypoxaemia ( $\text{PaO}_2 = 4.9$  kPa) on the third day postoperatively, reveal differences in several signals, of which lipids are the most significant (Fig. 1).

Since the metabolome mirrors environmental changes (Nicholson et al. 2002), we hypothesized that the disease could be reflected at the metabolic level on the first day postoperatively. Therefore, we screened for possible associations between the metabolome and the hypoxaemia

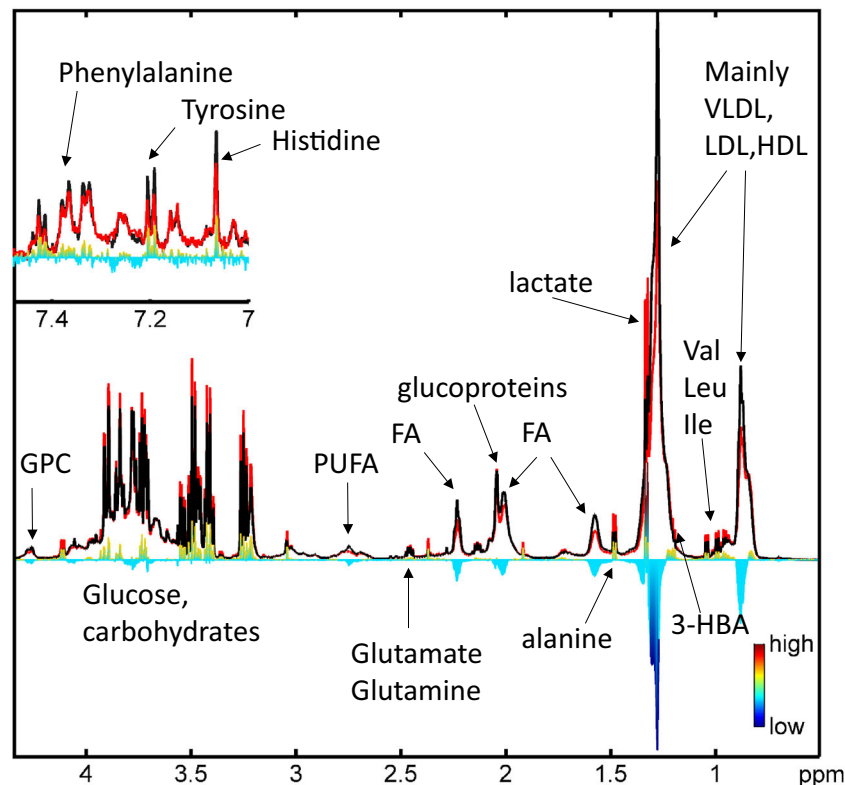


**Fig. 1** Serum metabolic fingerprints. Representative 1D CPMG  $^1\text{H}$ -NMR spectral profiles run on samples collected 16 h postoperatively of a patient not developing hypoxaemia (partial pressure of oxygen in arterial blood,  $\text{PaO}_2 = 10.7$  kPa) (black) and a patient showing hypoxaemia ( $\text{PaO}_2 = 4.9$  kPa) (red). The diagnosis was based on  $\text{PaO}_2$  measured 72 h after weaning from cardiopulmonary bypass (CPB). Spectral difference (unaffected—hypoxaemia) (red—yellow—blue colour coded) reveals metabolite fluctuations between the patients. Higher levels of signals from lipoproteins, fatty acids and lower levels of lactate, glucose, and some amino acids are observed in the hypoxaemia compared to unaffected patient. Using a combination of the NMR metabolic profiling database (BBIORFCODE, Bruker),

The Human Serum Metabolome Database (HMDB), and literature references, 63 resonances out of 64 were assigned to metabolites (Table 2, Supplementary). Spectra were internally calibrated to the  $-\text{CH}_3$  signal of lactate at chemical shift ( $\delta$ ) = 1.33 ppm. 1D one-dimensional, CPMG Carr–Purcell–Meiboom–Gill, VLDL very-low density lipoproteins, LDL low-density lipoproteins, HDL high-density lipoproteins, Val valine, Leu leucine, Ile isoleucine, 3-HBA 3-hydroxybutyric acid, FA fatty acids, PUFA polyunsaturated fatty acids, GPC glycerophosphocholine,  $\text{PaO}_2$  partial pressure of oxygen, kPa kilopascal, ppm parts per million, a.u. arbitrary units (Color figure online)

scores ( $\text{PaO}_2$ ) used in diagnosis (Table 1, Supplementary). Interestingly, PLS regression analysis revealed a strong correlation between the systemic and pulmonary phenotypes and  $\text{PaO}_2$  ( $R^2 = 0.97$ , Fig. 2a), indicating that serum NMR-based metabolomics can be used to screen for early signs of disease. Based on PLS results (Fig. 2a,b) we reasoned that subgrouping the 32 patients diagnosed with ALI into patients developing mild ( $8.4 > \text{PaO}_2 \geq 6.3$  kPa) and severe ( $\text{PaO}_2 < 6.2$  kPa) hypoxaemia, would provide better understanding of underlying mechanisms. Subsequently, the differences between the three groups (unaffected, mild, and severe hypoxaemia) were assessed by PLS-DA. The models displayed  $>95\%$  accuracy (Fig. 2c). The models were tested for some potentially influencing factors (Fig. 2d) that could obscure the accuracy of our proposed clinical test, and no significant interference was observed. The duration of anaesthesia, CABG, CPB, cross-clamp time, and fluid administration is

known to have an impact on patients' outcome postoperatively. Therefore, we attempted to correlate metabolic information with these intraoperative variables, but did not detect any strong association (cross-validated  $R^2$  values ranging between 0.14 and 0.51).

We also checked, whether common postoperative complications such as postoperative systemic inflammatory response syndrome (SIRS) and renal dysfunction, associate with the metabolome and confound the analysis. PLS yielded no association between the observed metabolic changes and indices of SIRS (measured as the levels of leucocytes; cross-validated  $R^2 = 0.17$  and CRP; cross-validated  $R^2 = 0.04$ ) and renal dysfunction (measured as creatinine concentration; cross-validated  $R^2 = 0.40$ ) measured 72 h postoperatively. This increases confidence that the metabolic linkage found is specific to hypoxaemia.

In summary, by collecting PA and LA blood samples 16 h after weaning from CPB, applying NMR and

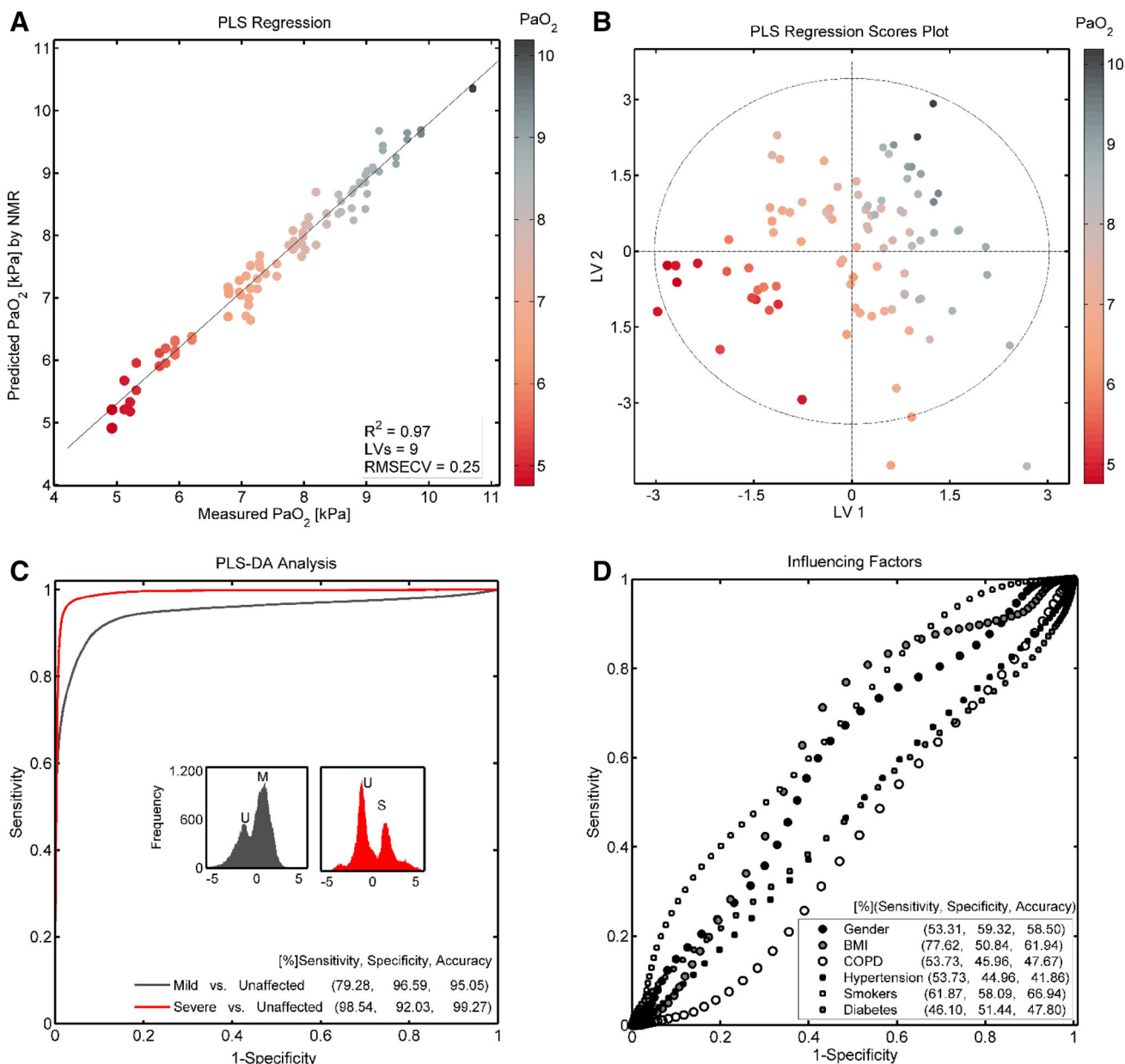


**Fig. 2** Metabolome screening reveals early signs of disease. Multivariate analysis was performed on spectra run on serum collected 16 h postoperatively from the left atrium and PA. Monte-Carlo validation was used for validation purpose (Methods 5). **a** Partial least-squares (PLS) regression reveals that NMR predicts the partial pressure of arterial O<sub>2</sub> (PaO<sub>2</sub>) measured three day postoperatively already the first morning post-CPB (predicted correlation R<sup>2</sup> = 0.97). Model robustness was assessed by repeating PLS modeling six times (R<sup>2</sup> = 0.97 ± 0.008, root-mean-square error of cross-validation RMSECV = 0.251 ± 0.034). **b** The first two latent variables (LVs) show patients clustering according to PaO<sub>2</sub>. Patients developing severe hypoxaemia (PaO<sub>2</sub> ≤ 6.2 kPa) cluster along -LV1; unaffected patients (PaO<sub>2</sub> > 8.5 kPa) cluster along +LV1; while mild hypoxaemia patients (8.4 > PaO<sub>2</sub> ≥ 6.3 kPa) cluster in-between. **c** Separation between Unaffected/Mild and Unaffected/Severe patients was

obtained through PLS-discriminant analysis (PLS-DA). Data was randomly split into a calibration (70 %) and validation set (30 %), and PLS-DA was performed with 5000 iterations. The frequency plots (gray and pink) show samples distributions from each group (U unaffected, M mild, S severe) used in the calibration set. Following PLS-DA, each patient’s predicted score was used to build the receiver operating characteristic (ROC) curve; each curve contains the results achieved from 5000 runs. Finally, PLS and PLS-DA models were further validated by 500× permuting the labels. No model was found over-fitted (p < 0.001). Sensitivity, specificity, and accuracy are given as percentages. **d** The possible influencing factors reveal no interference with the results (AUC < 0.67). BMI body mass index, COPD chronic obstructive pulmonary disease (Color figure online)

multivariate statistics, the hypoxaemia scores on the third day postoperatively could be predicted with a root-mean-squared error (RMSE) of 0.25 kPa (Fig. 2a).

### 3.2 Metabolic hallmark of postoperative hypoxaemia

The *fingerprints* or “*snapshots*” (Xia et al. 2013) of metabolism discerned in the screening process were investigated further. A total of 64 different metabolites were analyzed, of which one was unidentifiable (Supplementary Table 2). Perturbations in the levels of metabolites involved in normal cellular functioning (amino acids, carbohydrates, ketones), cellular signaling (1,2-diacylglycerol), inflammation (arachidonic and eicosapentaenoic acid), cell membrane and alveolar surfactant components (fatty acids, cholesterol, phospholipids) (Chen and Kolls 2010; Saxena 2005) were found crucial in the development of hypoxaemia (Fig. 3a). The contribution of each metabolite to modelling PaO<sub>2</sub> values was assessed by variables important in projection (VIPs) scores (Fig. 3b). Carnitine, arachidonic and eicosapentaenoic acid, glycoprotein, citrate, phenylalanine, glycine, plasmalogen, and lysophosphocholine (Lyso-PC), among others, showed highest scores, indicating their key roles in later outcomes. In addition, phospholipids and fatty acids (FA) showed highest fold changes in both hypoxaemia groups compared to the unaffected patients (Fig. 3b), indicating severe derangements in their pathways. Most metabolites showed consistent trends from none-to-mild-to-severe hypoxaemia (Fig. 3c), indicating their correlation to the degree of later pulmonary dysfunction and their possible function as predictive biomarkers. Finally, to understand the metabolic hallmark of hypoxaemia we have provided insights into the complex metabolic crosstalk in some of the affected paths (Fig. 3d), which have the potential to open up for promising therapeutic targets in the future.

### 3.3 Insights into the systemic and pulmonary phenotypes

While the exact origin of these metabolites is unknown, their release or disappearance from pulmonary (LA) and systemic (PA) vasculature may reflect their potential location. This disease is highly compartmentalized therefore knowing the origin of each metabolite would add new insights into translating its phenotypes.

In general, the same metabolic patterns were observed for both PA and LA samples with some exceptions, particularly for the severe hypoxaemia group (Fig. 4a, b, Supplementary Table 3). The levels of *N*-acetylated carbohydrates involved in the synthesis of glycoproteins and

glycolipids (Michal and Schomburg 2012) positively correlated with the severity of developing hypoxaemia. Also, an augmented extracellular supply of pyruvate, alanine, and citrate was observed in patients with hypoxaemia, especially in LA samples. Accumulation of ketone bodies [acetate, acetoacetate, 3-hydroxybutyrate (3-HBA)], carnitine, and FA were detected in hypoxaemia patients compared to unaffected patients. Increased levels of the inflammatory mediators (PUFA) together with accumulation of metabolites involved in cell membrane and surfactant production (phospholipids, cholesterol), seemed to be consistent in patients developing hypoxaemia. While PUFA levels were higher, cholesterol levels were lower in the pulmonary compared to the systemic circulation. Increased levels of triglyceride-rich lipoproteins and their breakdown products (free FA, di-, tri-acylglycerols, and glycerol) were observed in both PA and LA samples of the hypoxaemia patients. Decreased antioxidant levels (histidine, plasmalogen, and hypoxanthine) were observed only in the severe group with a tendency towards consumption by the pulmonary system. Finally, increased extracellular levels of osmoprotectants and cell volume regulators (glycine, glycerophosphocholine (GPC), and glutamate) were found in both PA and LA samples of the hypoxaemia patients. Collectively, these changes reflect a yet unraveled part of the complex pathophysiology and provide new insights into the multiple mechanisms involved in the progression to, or protection from, hypoxaemia post-CPB.

### 3.4 Early markers for hypoxaemia

A list of several metabolites is not ideal for developing cost-effective diagnostic tests, and due to general lack of hospital NMR instrumentation, diagnosis based on fewer metabolites would be more convenient, if they provide sufficient information to generate robust clinical models. Therefore, we have explored all metabolites individually or as ratios between metabolites and found powerful predictive markers. Several serum metabolites measured 16 h postoperatively were found significantly correlated to PaO<sub>2</sub> measured 72 h after weaning from CPB (Fig. 5a, Supplementary Table 4) and several showed strong predictive power for mild and severe hypoxaemia with high (AUC > 0.8, *p* < 0.0001) (Fig. 5b, Table 5 Supplementary).

## 4 Discussion

This is the first study of its kind, exploring metabolic changes on the first postoperative day following cardiac surgery with the use of CPB in patients at-risk of developing pulmonary dysfunction with hypoxaemia. We have



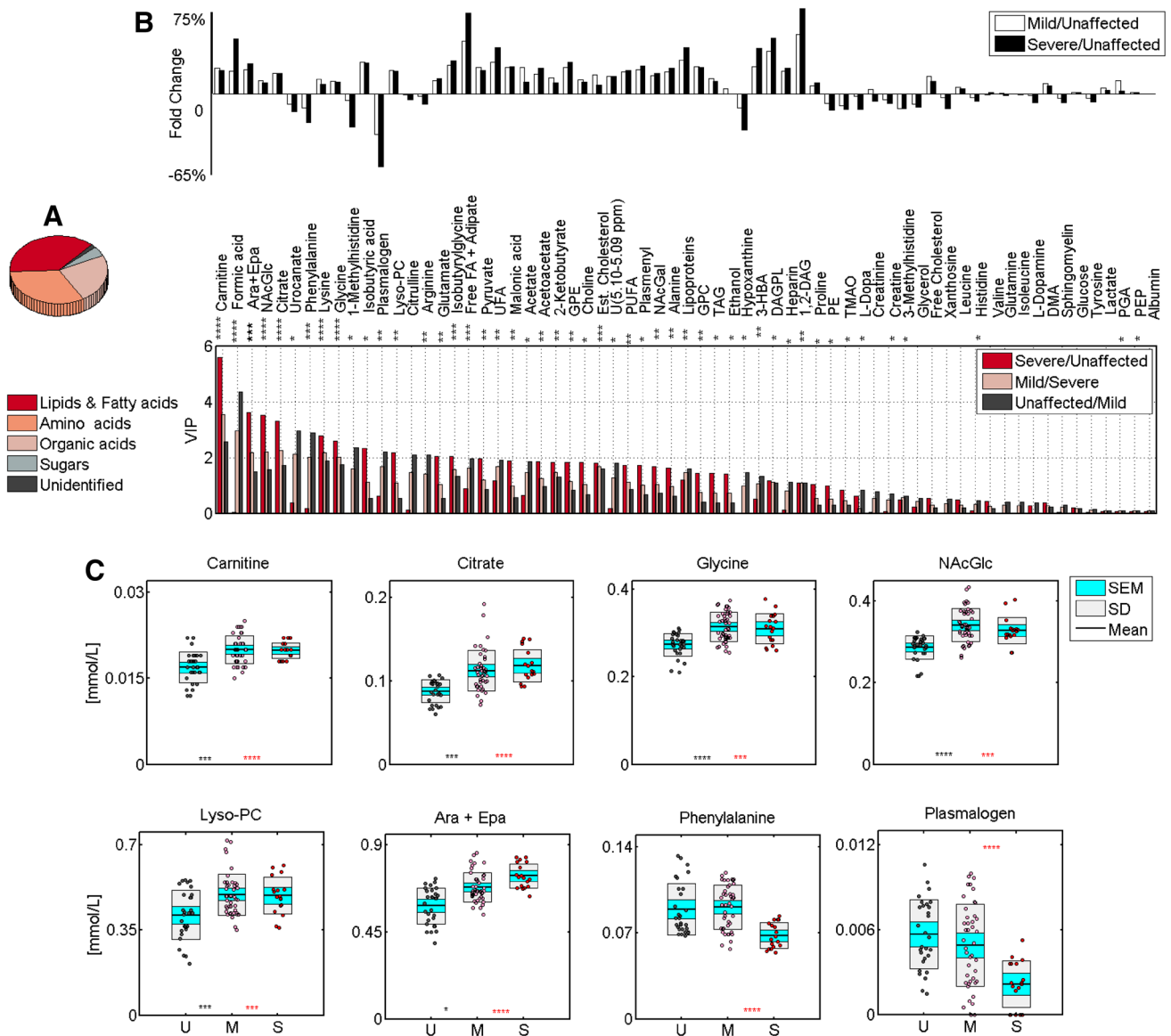


**Fig. 3** Metabolic hallmark of hypoxaemia. **a** Metabolites found contributing to the progression into postoperative hypoxaemia. **b** The importance of each metabolite in the progression was assessed by variable importance in projection (VIP) scores. The greater the score, the more influential the metabolite; VIP scores > 1 indicate important metabolites in predicting later outcomes, whereas VIP scores < 0.5 indicate less important metabolites. Metabolic fold changes were calculated as percent change in mean between mild and severe vs. unaffected patients ((M - U)/U)\*100, where M is mild, U is unaffected). Metabolite labelled with asterisk were found varying significantly between groups, by using ANOVA or its nonparametric analogue Kruskal-Wallis test (\*0.09 > p ≥ 0.01, \*\*10<sup>-2</sup> > p ≥ 10<sup>-3</sup>, \*\*\*10<sup>-4</sup> > p ≥ 10<sup>-5</sup>, \*\*\*\*p < 10<sup>-5</sup>). **c** Concentration distribution of some of the most discerning metabolites; SD standard deviation, SEM standard error of mean, U unaffected, M mild, S severe, Asterisks black significant difference between

unaffected and mild, red significant difference between unaffected and severe. **d** Simplified metabolite pathways. Only identified and quantified metabolites are colored (blue higher concentration, green lower concentration in hypoxaemia compared to unaffected patients), whilst unidentified metabolites in the same pathways are in grey. *NAcGlc* N-acetylglucosamine, *Ara + Epa* arachidonic acid (Ara, 20:4 ω-6) and Eicosapentaenoic acid (Epa, 20:5 ω-3), *Lyso-PC* lysophosphatidylcholine, *FA* fatty acids; *UFA* unsaturated fatty acids, *GPE* glycerophosphoethanolamine, *Est.* esterified, *U* unidentified, *PUFA* polyunsaturated fatty acids, *NAcGal* N-acetylgalactosamine, *GPC* glycerophosphocholine, *TAG* triacylglycerol, *3-HBA* 3-hydroxybutyric acid, *DAGPL* diacylglycerophospholipid, *1,2-DAG* 1,2-diacylglycerol, *PE* phosphoethanolamine, *TMAO* trimethylamine-N-oxide, *PGA* phosphoglyceric acid, *PEP* phosphoenolpyruvate (Color figure online)

demonstrated that the metabolome changes so dramatically that the degree of hypoxaemia can be predicted at least 2 days before the clinical diagnosis.

NMR spectra (Fig. 1) and multivariate modelling accurately related perturbations in the metabolome recorded first morning postoperatively with later diagnostic

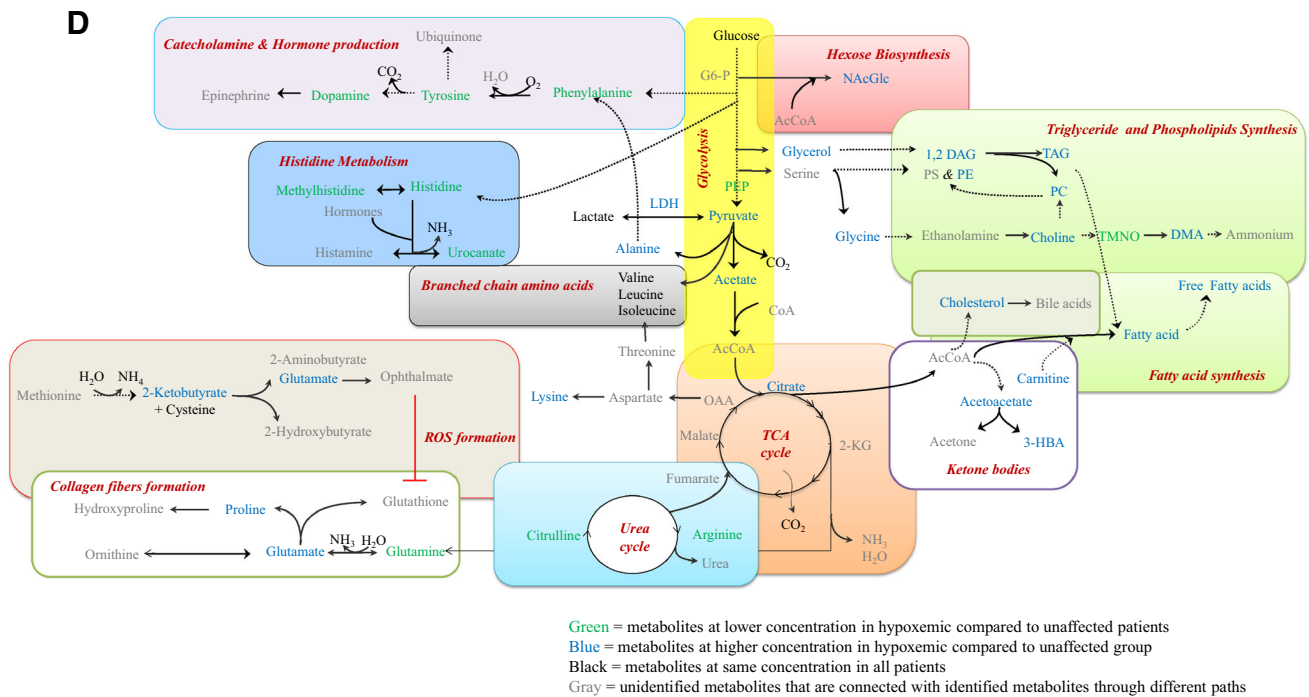
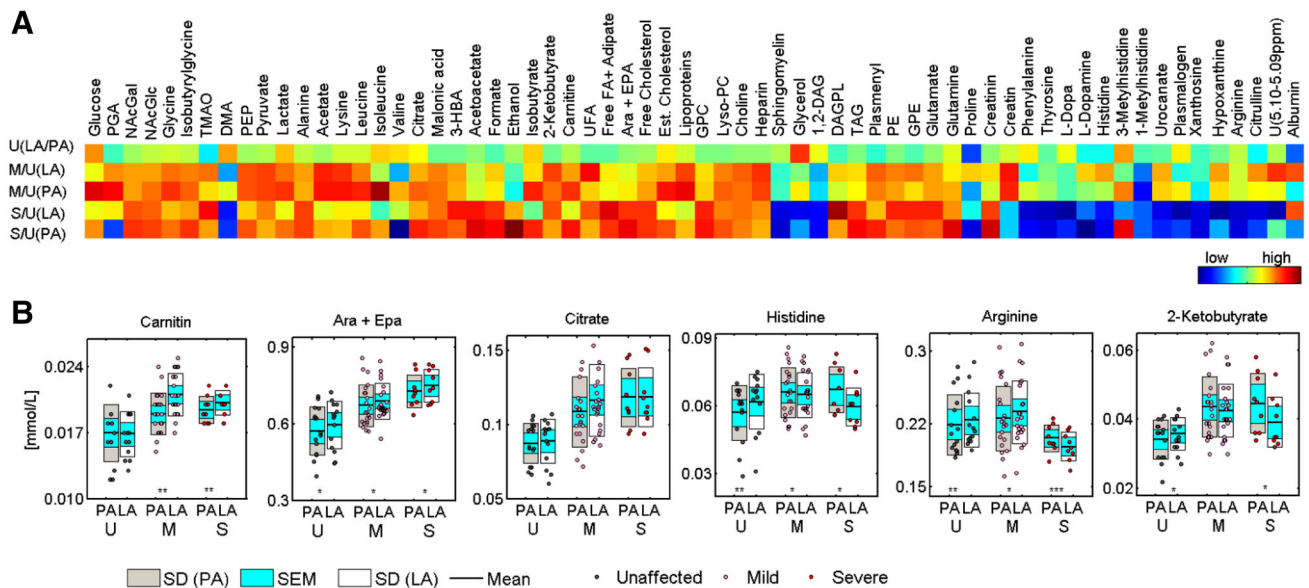
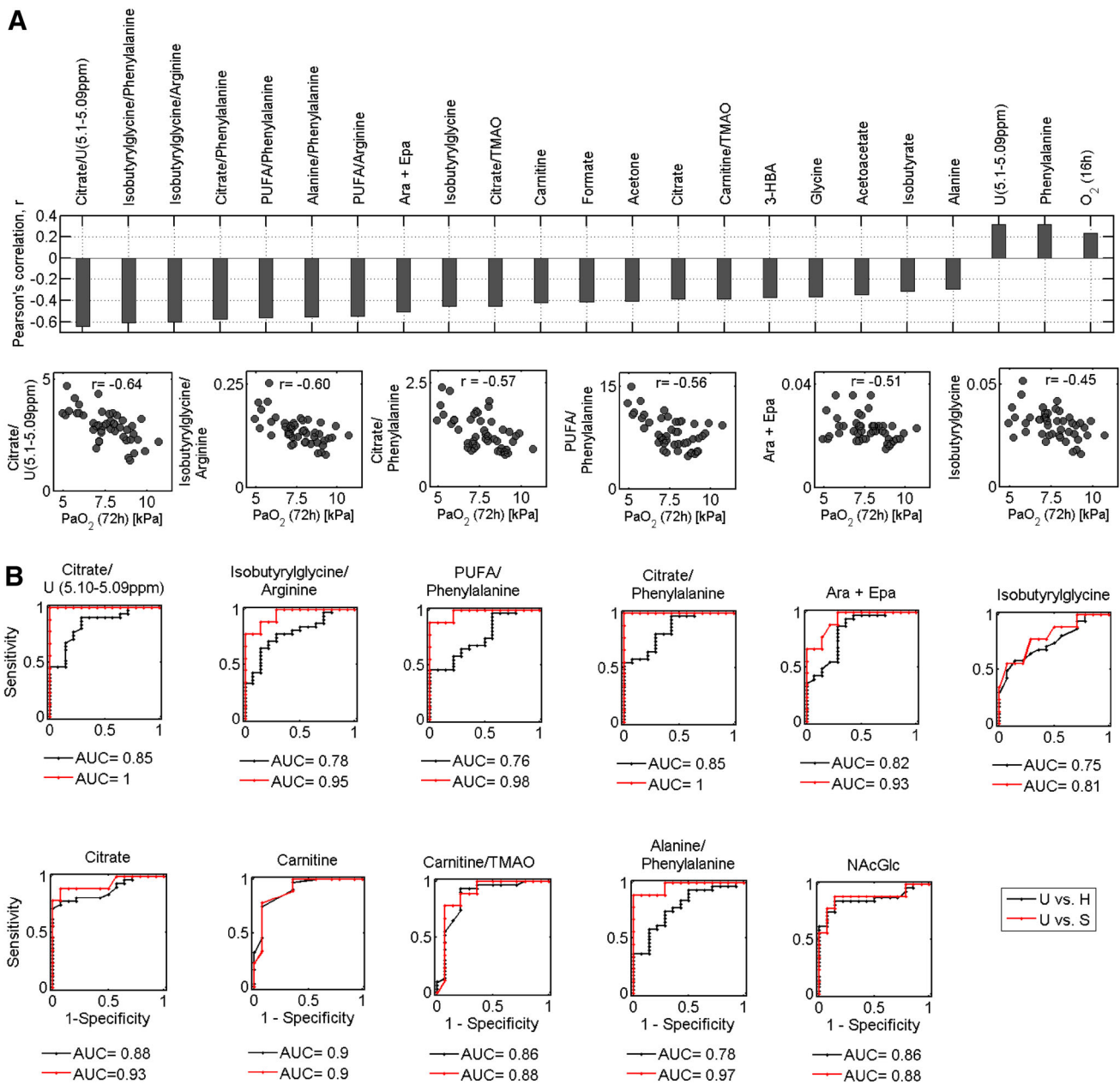


Fig. 3 continued



**Fig. 4** Systemic versus pulmonary phenotypes. To understand what happens during the short passage from heart-to-lung-to-heart, the pair *t* test or its nonparametric analogue Wilcoxon-signed rank sum test (depending on the data distribution) were used to check for differences between left atrial (LA) and pulmonary artery (PA) samples in each group. **a** Heat map visualization depicts the metabolic abundances between LA and PA samples in the hypoxaemia groups compared to unaffected patients (blue higher levels in hypoxaemia compared to unaffected patients; red lower levels in hypoxaemia compared to unaffected patients). Of 64 metabolites, 43 varied between LA and PA samples in at least one group (Table 3, Supplementary). **b** For example, higher levels of carnitine and

arachidonic acid were found leaving the lungs in both mild and severe hypoxaemia patients; while histidine and arginine were found to be consumed by the pulmonary system (lower levels in LA samples) in the severe acute lung injury group but not in the mild hypoxaemia nor in the unaffected group. Additionally, citrate was significantly increased in both mild and severe hypoxaemia groups compared to unaffected group, however, its levels were found unchanged when LA samples were compared to PA samples. Asterisks: \*0.09 > p ≥ 0.01, \*\*10<sup>-2</sup> > p ≥ 10<sup>-3</sup>, \*\*\*10<sup>-4</sup> > p ≥ 10<sup>-5</sup>. SD standard deviation, SEM standard error of mean, U unaffected, M mild, S severe; for metabolite abbreviations see Fig. 3 (Color figure online)



**Fig. 5** Biomarkers predict progression into hypoxaemia after cardiac surgery 2 days before clinical diagnosis. **a** The relation between serum metabolites (either alone or as ratio between two metabolites) measured first morning (exactly 16 h) after weaning from CPB and the PaO<sub>2</sub> values measured on day 3 postoperative was calculated by Pearson's correlation coefficient (Pearson's  $r$ ) (Table 4, Supplementary). Examples of scatter plots are illustrated, showing correlation between left atrial-derived metabolites and PaO<sub>2</sub> (Pearson's  $r = 0.45$ – $0.64$ ,  $p < 0.001$ ). Additionally, the relation between blood

O<sub>2</sub> measured 16 h and the PaO<sub>2</sub> measured on day 3 after surgery is shown, indicating no significant correlation (Pearson's  $r = 0.264$ ,  $p = 0.08$ ). **(b)** We calculated the area under the curve (AUC) for each biomarker candidate (Table 5, Supplementary), and, among others, citrate, phenylalanine, carnitine, TMAO, Ara + Epa, isobutyrylglycine, PUFA, alanine, and NAcGlc were identified as powerful predictive markers of later outcome. *U* unaffected, *H* hypoxaemia (all mild and severe patients), *S* severe. For metabolite abbreviations see Fig. 3

scores (Fig. 2a, b). It is noteworthy that the metabolome not only contained information about the future degree of oxygenation impairment 2 days later, but could also accurately differentiate mild and severe hypoxaemia from unaffected patients with 79.3 and 98.5 % sensitivity, and

96.6 and 92 % specificity, respectively (Fig. 2c). While some of these findings have previously been reported occurring in patients diagnosed with acute lung injury or acute respiratory distress syndrome (Evans et al. 2014; Serkova et al. 2008; Stringer et al. 2011), we report

metabolic changes occurring before the clinical signs of hypoxaemia.

From PA and LA samples, several metabolites were observed to vary between patients (Fig. 3 and 4). Of these, several markers significantly correlated with PaO<sub>2</sub> ( $p \leq 0.05$ ) (Fig. 5a,b). These are markers of antioxidant status and peroxidation (histidine, plasmalogen, PUFA); ATP depletion and reactive oxygen species (ROS) formation (citrate); inflammation [arachidonic and eicosapentaenoic acid, 1,2-diacylglycerol (1,2-DAG)]; changes in osmotic and cell-volume regulation (glycine); membrane injury (phospholipids); and mitochondrial dysfunction (carnitine). The use of metabonomics predicting postoperative hypoxaemia with AUC and detection rates as described here has not been reported before.

The range of changes found in this study, from carbohydrates to amino acids, ketone bodies, FA, and phospholipids adds information to the present knowledge of the pathophysiology leading to hypoxaemia induced by an indirect insult to the lungs by cardiac surgery with use of CPB. The metabolic manifestations of mild and severe hypoxaemia compared to the unaffected patients appear to be similar, indicating the existence of common pathways. Therefore, knowledge of the core pathways and their interconnections may help us understanding the pathogenesis. The role of each metabolite and its connection to other metabolites in the human body is far from being fully understood. Nevertheless, in the following, we try to combine our observed alterations with possible roles of single metabolites into a model of intracellular processes leading up to hypoxaemia.

We observed altered metabolite levels down-stream of glucose metabolism. Pyruvate, alanine, and tricarboxylic acid (TCA) metabolite levels positively correlated with the severity of hypoxaemia. Their levels were higher in the pulmonary circulation (LA) compared to the systemic circulation (PA), indicating that pulmonary cells release these metabolites. This suggests an impaired oxidative phosphorylation in the lung tissue. In line with these observations, our results confirm previous studies conducted on plasma (Stringer et al. 2011) and bronchoalveolar lavage fluid (BALF) (Evans et al. 2014) samples collected from patients diagnosed with acute lung injury, in which the levels of TCA metabolites were found to be increased. Increased TCA levels were also found predicting the progression from SIRS to multiple organ failure in critically ill patients (Mao et al. 2009) and in predicting sepsis outcomes (Langley et al. 2013). Carnitine, normally found in mitochondria, helping FA delivery for  $\beta$ -oxidation, was significantly increased in LA samples of patients with hypoxaemia, which may also indicate impaired oxidative phosphorylation and a possible leakage into the bloodstream. Supporting this, isobutyrylglycine, a marker of

impaired mitochondrial FA  $\beta$ -oxidation, was also associated with severity of hypoxaemia. Mitochondrial impairments enhance oxidative stress (Jana et al. 2013), causing alveolar cell death (Chow et al. 2003). Under homeostatic conditions, however, various antioxidants are capable of alleviating the damaging effects of ROS from the system (Scheibmeir et al. 2005), but an insufficient antioxidant barrier cannot counteract this damage. Low levels of the antioxidants histidine, urocanate, and plasmalogen in patients with severe hypoxaemia, in contrast to the mildly affected patients, may indicate an inefficient scavenging ability leading to a continued ROS presence, especially in the pulmonary microenvironment. The lower histidine levels in LA samples of the severely affected group may indicate an increased pulmonary demand to counteract peroxidation events. In addition, we found lower levels of the antioxidant hypoxanthine in patients developing hypoxaemia. Interestingly, previous metabonomics work conducted by Evans and co-workers on BALF of patients diagnosed with the severe lung injury form acute respiratory distress syndrome revealed a 41 fold increased in hypoxanthine levels compared to healthy subjects (Evans et al. 2014). Our results may be complementary to their findings, as hypoxanthine may diffuse in the lungs early in the stage of pulmonary dysfunction, and may accumulate later in the stage of full blown disease. To verify this hypothesis other studies involving both blood and BALF samples collected at different time points during disease progression should be performed.

It has been demonstrated that 2-hydroxybutyric acid is an early marker of increased lipid oxidation (Nishiumi et al. 2012). Membrane bound phospholipids and PUFA are susceptible to oxidation leading to the formation of highly reactive hydroperoxides (Crader and Repine 2012). These react with many biochemical substances having enormous impacts on normal cellular functioning, including endothelial activation and surfactant phospholipid disruption. In this study, the levels of PUFA and adipic acid (a byproduct of peroxidation (Jana et al. 2013) were found correlating with later pulmonary dysfunction, whereas plasmalogen (implicated in protection against ROS and peroxynitrite formation (Zoeller et al. 2002) levels were decreased, especially in the severe hypoxaemia group.

The ketogenic capacity (3-HBA, acetoacetate, and acetate) positively correlated with progression of hypoxaemia, and elevated levels are known to be indices of inadequate energy supply, or poor metabolism, leading to excessive triglyceride and fatty acid breakdown. This may partially explain the increased levels of circulating free FA, glycerol, triacylglycerol, and lipoproteins in both PA and LA samples of patients with hypoxaemia. Choline, phospholipids, 1,2-DAG, PUFA, and cholesterol are essential for structural integrity and cell membrane signaling. An



increase in their levels reflects an activation of the protective mechanism and a possible structural derangement in patients progressing into disease. Lipids are highly interconnected signaling molecules that regulate metabolic, innate immune and inflammatory processes, and alteration in one lipid will automatically trigger major deregulation in several signaling pathways causing profound physiological responses (Wymann and Schneider 2008). The levels of arachidonic and eicosapentaenoic acids were higher in patients with hypoxaemia, especially in LA samples, indicating an increased inflammatory environment. These PUFA may be released by activation of phospholipase A<sub>2</sub>, hydrolyzing membrane glycerophospholipids (Wymann and Schneider 2008), which may also indicate cell membrane injury. According to Wymann and Schneider, accumulation of diacylglycerols activates protein kinases, increases production of ROS and oxidative stress, and induces the synthesis of pro-inflammatory cytokines. Because one of the characteristics of this disease is dysfunction of alveolar surfactants, the increased levels of some phospholipids, especially in LA samples of hypoxaemia patients, may also be partly explained by surfactant leakage, which could indicate a damaged endothelial-alveolar barrier.

Interestingly, decreased arginine and citrulline levels were observed in the group developing severe hypoxaemia, especially in the pulmonary circulation. In fact, blood arginine depletion has previously been linked to ALI (Murakami et al. 2007; Naz et al. 2013), sepsis (Murakami et al. 2007) and cystic fibrosis (Luiking et al. 2005), and supplementation of arginine was observed to reduce inflammation (Murakami et al. 2007). The deficiency of arginine was not due to lack of metabolites involved in its synthesis, as lysine, glutamate, and proline levels were increased in these patients. During stress responses, blood lysine levels are known to increase to reduce oxidative stress (Jana et al. 2013). The increased levels of lysine observed especially in LA samples from hypoxaemia patients may reflect an attempt to counteract oxidative stress. In addition, dimethylamine (DMA) was elevated in sick patients. DMA is synthesized from asymmetric dimethylarginine, the endogenous inhibitor of NO synthesis, and an increased level of this metabolite may result in accumulation of ROS and reactive nitrogen species contributing to lung dysfunctions (Naz et al. 2013).

N-Acetylated carbohydrates involved in synthesis of glycolipids and glycoproteins (Michal and Schomburg 2012) were also found positively correlating with the disease. These acids are part of the pentose metabolism, which is known to be more active under stress (Zachara et al. 2004), especially under hypotonic stress conditions. Interestingly, the osmolytes counteracting cellular swelling (GPC, glutamate, and glycine) were elevated in

hypoxaemia patients, probably indicating activated mechanisms involved in cell-volume regulation and the prevention of cell death (Naguro et al. 2012).

Thus, our findings suggest increased glucose metabolism, defects in the mitochondrial respiratory system affecting ROS generation, impaired antioxidant state, increased peroxidation and oxidative stress, cell membrane derangements, cellular swelling and cell damage in patients developing hypoxaemia.

It is important to bear in mind that some of above mentioned mechanisms are still not proven beyond doubt, hence the discussed metabolic considerations and consequences are somewhat hypothetical, yet plausible to explain important derangements leading to hypoxaemia. Based on our findings, the serum metabolome seems to reflect not only metabolic changes in the systemic but also in the pulmonary responses to later hypoxaemia. However, as these changes are minimal, they may not fully reflect the impairments occurring in the lungs. Including metabolomics analysis performed on BALF samples may therefore add further insights into the metabolic changes in the lungs.

Regarding our study design, there are some limitations. The small sample size, especially in the severe hypoxaemia patients, may bias the results. The fact that we achieved similar results in LA and PA samples offers to some extent confidence in data validity, however, the results must be verified in larger studies. We used serum samples for the analyses. Since the coagulation processes take some time, the samples were left half an hour at ambient temperature before centrifugation. In this period metabolic changes may have occurred. However, all samples were treated equally and, therefore, the differences between samples can be expected to reflect the true changes in the patients. In addition, blood metabolite levels might not fully reflect changes in intracellular metabolism. Regarding the choice of methodology, despite the robustness and informative nature of NMR, the technique suffers from low sensitivity and signal overlap impeding identification of metabolites occurring at low concentrations, and therefore, some potentially important changes were not detected. In the future, collecting different biological matrices and analyzing samples by both NMR and e.g. mass spectrometry-based approaches would add more insights to the pathogenesis of postoperative pulmonary dysfunctions.

## 5 Conclusion

In conclusion, by mapping metabolic perturbations at an early stage, we have identified metabolite hallmarks of hypoxaemia, which may bridge the gap between pathogenesis and full-blown disease. Markers such as

arachidonic and eicosapentaenoic acid, citrate, carnitine, glycine, phenylalanine, arginine, and histidine serve as central nodes in their metabolism and therefore have a high impact in predicting disease progression. No single metabolite captured the complexity of hypoxaemia alone, as different pathways simultaneously showed imbalances. Therefore, to prevent early progression into hypoxaemia, therapeutics targeting several pathways may be more effective.

**Acknowledgement** The study was financed by Aalborg University Hospital and Aalborg University. The NMR laboratory at Aalborg University is supported by the Obel, SparNord and Carlsberg Foundations.

#### Compliance with ethical standards

**Conflict of interest** R.G.M, B.S.R., M.A.H., S.R.K., S.P. and R.W. have filed a patent application for some of the metabolic biomarkers described in the manuscript and for an algorithm predicting the condition from experimental data.

**Ethical approval** The study was approved by the regional ethical committee (N-20080016).

**Informed consent** After oral as well as written informed consent was obtained, patients scheduled for elective coronary artery bypass grafting (CABG) were included.

#### References

- Apostolakis, E., Filos, K. S., Koletsis, E., & Dougenis, D. (2009). Lung dysfunction following cardiopulmonary bypass. *Journal of Cardiac Surgery*, 25(1), 47–55.
- Bhargava, M., & Wendt, C. H. (2012). Biomarkers in acute lung injury. *Translational Research*, 159(4), 205–217.
- Campbell, R. (2010). notBoxPlot.
- Chen, K., & Kolls, J. K. (2010). Good and bad lipids in the lung. *Nature Medicine*, 16(10), 1078–1079.
- Chow, C.-W., Herrera Abreu, M. T., Suzuki, T., & Downey, G. P. (2003). Oxidative stress and acute lung injury. *American Journal of Respiratory Cell and Molecular Biology*, 29(4), 427–431.
- Clark, S. C. (2006). Lung injury after cardiopulmonary bypass. *Perfusion*, 21(4), 225–228.
- Crader, M., & Repine, J. D. (2012). Breath biomarkers and the acute respiratory distress syndrome. *Journal of Pulmonary & Respiratory Medicine*, 02(01), 1–9.
- De Backer, D., Creteur, J., Zhang, H., Norrenberg, M., & Vincent, J. L. (1997). Lactate production by the lungs in acute lung injury. *American Journal of Respiratory and Critical Care Medicine*, 156(4 Pt 1), 1099–1104.
- Eriksson, I., Johansson, E., Kettaneh-Wold, N., & Wold, S. (2001). *Multi- and megavariate data analysis. Principles and applications*. Umeå: Umetrics Academy.
- Evans, C. R., Karnovsky, A., Kovach, M. A., Standiford, T. J., Burant, C. F., & Stringer, K. A. (2014). Untargeted LC-MS metabolomics of bronchoalveolar lavage fluid differentiates acute respiratory distress syndrome from health. *Journal of Proteome Research*, 13(2), 640–649.
- Fremont, R. D., Koyama, T., Calfee, C. S., Wu, W., Dossett, L. A., Bossert, F. R., et al. (2010). Acute lung injury in patients with traumatic injuries: Utility of a panel of biomarkers for diagnosis and pathogenesis. *The Journal of Trauma*, 68(5), 1121–1127.
- Gajic, O., Dabbagh, O., Park, P. K., Adesanya, A., Chang, S. Y., Hou, P., et al. (2011). Early identification of patients at risk of acute lung injury: Evaluation of lung injury prediction score in a multicenter cohort study. *American Journal of Respiratory and Critical Care Medicine*, 183(4), 462–470.
- Good, P. I. (2011). *Analyzing the large number of variables in biomedical and satellite imagery*. Hoboken: Wiley.
- Jana, S. K., Dutta, M., Joshi, M., Srivastava, S., Chakravarty, B., & Chaudhury, K. (2013). 1H NMR based targeted metabolite profiling for understanding the complex relationship connecting oxidative stress with endometriosis. *BioMed Research International*, 2013, 329058.
- Kominsky, D. J., Campbell, E. L., & Colgan, S. P. (2010). Metabolic shifts in immunity and inflammation. *Journal of Immunology (Baltimore, Md.: 1950)*, 184(8), 4062–4068.
- Langley, R. J., Tsalik, E. L., van Velkinburgh, J. C., Glickman, S. W., Rice, B. J., Wang, C., et al. (2013). An integrated clinico-metabolomic model improves prediction of death in sepsis. *Science Translational Medicine*, 5(195), 195ra95.
- Levitt, J. E., Gould, M. K., Ware, L. B., & Matthay, M. A. (2009). The pathogenetic and prognostic value of biologic markers in acute lung injury. *Journal of Intensive Care Medicine*, 24(3), 151–167.
- Li, H., Liang, Y., Xu, Q., & Cao, D. (2009). Key wavelengths screening using competitive adaptive reweighted sampling method for multivariate calibration. *Analytica Chimica Acta*, 648(1), 77–84.
- Luiking, Y. C., Poeze, M., Ramsay, G., & Deutz, N. E. P. (2005). The role of arginine in infection and sepsis. *Journal of Parenteral and Enteral Nutrition*, 29(1 suppl), S70–S74.
- Mao, H., Wang, H., Wang, B., Liu, X., Gao, H., Xu, M., et al. (2009). Systemic metabolic changes of traumatic critically ill patients revealed by an NMR-based metabolomic approach. *Journal of Proteome Research*, 8(12), 5423–5430.
- Matthay, M. A., Ware, L. B., & Zimmerman, G. A. (2012). The acute respiratory distress syndrome. *The Journal of Clinical Investigation*, 122(8), 2731–2740.
- Matthay, M. A., & Zimmerman, G. A. (2005). Acute lung injury and the acute respiratory distress syndrome: Four decades of inquiry into pathogenesis and rational management. *American Journal of Respiratory Cell and Molecular Biology*, 33(4), 319–327.
- Meiboom, S., & Gill, D. (1958). Modified spin-echo method for measuring nuclear relaxation times. *Review of Scientific Instruments*, 29(8), 688.
- Michal, G., & Schomburg, D. (2012). *Biochemical pathways: An atlas of biochemistry and molecular biology*. p. 54, (G. Michal & D. Schomburg, Eds.) (2nd ed.). New York: Wiley.
- Milot, J., Perron, J., Lacasse, Y., Létoirneau, L., Cartier, P. C., & Maltais, F. (2001). Incidence and predictors of ARDS after cardiac surgery. *Chest*, 119(3), 884–888.
- Murakami, K., Enkhbaatar, P., Yu, Y.-M., Traber, L. D., Cox, R. A., Hawkins, H. K., et al. (2007). L-arginine attenuates acute lung injury after smoke inhalation and burn injury in sheep. *Shock (Augusta, Ga.)*, 28(4), 477–483.
- Naguro, I., Umeda, T., Kobayashi, Y., Maruyama, J., Hattori, K., Shimizu, Y., et al. (2012). ASK3 responds to osmotic stress and regulates blood pressure by suppressing WNK1-SPAK/OSR1 signaling in the kidney. *Nature Communications*, 3, 1285.
- Naz, S., Garcia, A., Rusak, M., & Barbas, C. (2013). Method development and validation for rat serum fingerprinting with CE-MS: Application to ventilator-induced-lung-injury study. *Analytical and Bioanalytical Chemistry*, 405(14), 4849–4858.
- Ng, C. S. H., Wan, S., Yim, A. P. C., & Arifi, A. A. (2002). Pulmonary dysfunction after cardiac surgery. *Chest*, 121(4), 1269–1277.

- Nicholson, J. K., Connelly, J., Lindon, J. C., & Holmes, E. (2002). Metabonomics: A platform for studying drug toxicity and gene function. *Nature Reviews Drug Discovery*, 1(2), 153–161.
- Nicholson, J. K., Lindon, J. C., & Holmes, E. (1999). “Metabonomics”: Understanding the metabolic responses of living systems to pathophysiological stimuli via multivariate statistical analysis of biological NMR spectroscopic data. *Xenobiotica; The Fate of Foreign Compounds in Biological Systems*, 29(11), 1181–1189.
- Nishiumi, S., Kobayashi, T., Ikeda, A., Yoshie, T., Kibi, M., Izumi, Y., et al. (2012). A novel serum metabolomics-based diagnostic approach for colorectal cancer. *PLoS One*, 7(7), e40459.
- Norgaard, L., Saudland, A., Wagner, J., Nielsen, J. P., Munck, L., & Engelsen, S. B. (2000). Interval partial least-squares regression (iPLS): A comparative chemometric study with an example from near-infrared spectroscopy. *Applied Spectroscopy*, 54(3), 413–419.
- Obuchowski, N. A., Lieber, M. L., & Wians, F. H. (2004). ROC curves in clinical chemistry: Uses, misuses, and possible solutions. *Clinical Chemistry*, 50(7), 1118–1125.
- Oeckler, R. A., & Hubmayr, R. D. (2008). Cell wounding and repair in ventilator injured lungs. *Respiratory Physiology & Neurobiology*, 163(1–3), 44–53.
- Perl, M., Lomas-Neira, J., Venet, F., Chung, C.-S., & Ayala, A. (2011). Pathogenesis of indirect (secondary) acute lung injury. *Expert Review of Respiratory Medicine*, 5(1), 115–126.
- Rasmussen, B. S., Laugesen, H., Sollid, J., Grønland, J., Rees, S. E., Toft, E., et al. (2007). Oxygenation and release of inflammatory mediators after off-pump compared with after on-pump coronary artery bypass surgery. *Acta Anaesthesiologica Scandinavica*, 51(9), 1202–1210.
- Reiss, L. K., Uhlig, U., & Uhlig, S. (2012). Models and mechanisms of acute lung injury caused by direct insults. *European Journal of Cell Biology*, 91(6–7), 590–601.
- Rogers, A. J., & Matthay, M. A. (2014). Applying metabolomics to uncover novel biology in ARDS. *American Journal of Physiology. Lung Cellular and Molecular Physiology*, 306(11), L957–961.
- Routsi, C., Bardouniotou, H., Delivoria-Ioannidou, V., Kazi, D., Roussos, C., & Zakynthinos, S. (1999). Pulmonary lactate release in patients with acute lung injury is not attributable to lung tissue hypoxia. *Critical Care Medicine*, 27(11), 2469–2473.
- Rubinfeld, G. D., & Herridge, M. S. (2007). Epidemiology and outcomes of acute lung injury. *Chest*, 131(2), 554–562.
- Savorani, F., Tomasi, G., & Engelsen, S. B. (2010). icoshift: A versatile tool for the rapid alignment of 1D NMR spectra. *Journal of Magnetic Resonance (San Diego, Calif.: 1997)*, 202(2), 190–202.
- Saxena, S. (2005). Lung surfactant. *Resonance*, 10(8), 91–96.
- Scheibmeir, H. D., Christensen, K., Whitaker, S. H., Jegaethesan, J., Clancy, R., & Pierce, J. D. (2005). A review of free radicals and antioxidants for critical care nurses. *Intensive & Critical Care Nursing*, 21(1), 24–28.
- Serkova, N., Van Rheen, Z., Tobias, M., Pitzer, J., Wilkinson, J., & Stringer, K. (2008). Utility of magnetic resonance imaging and nuclear magnetic resonance-based metabolomics for quantification of inflammatory lung injury. *AJP*, 295(1), L152–L161.
- Shlomi, T., Cabili, M. N., & Ruppini, E. (2009). Predicting metabolic biomarkers of human inborn errors of metabolism. *Molecular Systems Biology*, 5, 263.
- Singh, N. P., Vargas, F. S., Cukier, A., Terra-Filho, M., Teixeira, L. R., & Light, R. W. (1992). Arterial blood gases after coronary artery bypass surgery. *Chest*, 102(5), 1337–1341.
- Stephens, R. S., Shah, A. S., & Whitman, G. J. R. (2013). Lung injury and acute respiratory distress syndrome after cardiac surgery. *The Annals of Thoracic Surgery*, 95(3), 1122–1129.
- Stringer, K. A., Serkova, N. J., Karnovsky, A., Guire, K., Paine, R., & Standiford, T. J. (2011). Metabolic consequences of sepsis-induced acute lung injury revealed by plasma 1H-nuclear magnetic resonance quantitative metabolomics and computational analysis. *American Journal of Physiology*, 300(1), L4–L11.
- Ware, L. B., Koyama, T., Billheimer, D. D., Wu, W., Bernard, G. R., Thompson, B. T., et al. (2010). Prognostic and pathogenetic value of combining clinical and biochemical indices in patients with acute lung injury. *Chest*, 137(2), 288–296.
- Weissman, C. (2004). Pulmonary complications after cardiac surgery. *Seminars in Cardiothoracic and Vascular Anesthesia*, 8(3), 185–211.
- Wheeler, A. P., & Bernard, G. R. (2007). Acute lung injury and the acute respiratory distress syndrome: A clinical review. *Lancet (London, England)*, 369(9572), 1553–1564.
- Wishart, D. S., Tzur, D., Knox, C., Eisner, R., Guo, A. C., Young, N., et al. (2007). HMDB: The Human Metabolome Database. *Nucleic Acids Research*, 35(Database issue), D521–526.
- Wold, S., Martens, H., & Wold, H. (1983). Matrix Pencils. In B. Kågström & A. Ruhe (Eds.), (Vol. 973, pp. 286–293). Berlin: Springer Berlin Heidelberg.
- Wold, S., Ruhe, A., Wold, H., & Dunn, W. J. I. I. (1984). The collinearity problem in linear regression. the partial least squares (PLS) approach to generalized inverses. *SIAM Journal on Scientific and Statistical Computing*, 5(3), 735–743.
- Wold, S., Sjöström, M., & Eriksson, L. (2001). PLS-regression: a basic tool of chemometrics. *Chemometrics and Intelligent Laboratory Systems*, 58, 109–130.
- Wymann, M. P., & Schneider, R. (2008). Lipid signalling in disease. *Nature Reviews Molecular Cell Biology*, 9(2), 162–176.
- Xia, J., Broadhurst, D. I., Wilson, M., & Wishart, D. S. (2013). Translational biomarker discovery in clinical metabolomics: An introductory tutorial. *Metabolomics*, 9(2), 280–299.
- Zachara, N. E., O'Donnell, N., Cheung, W. D., Mercer, J. J., Marth, J. D., & Hart, G. W. (2004). Dynamic O-GlcNAc modification of nucleocytoplasmic proteins in response to stress. A survival response of mammalian cells. *The Journal of biological chemistry*, 279(29), 30133–30142.
- Zoeller, R. A., Grazia, T. J., LaCamera, P., Park, J., Gaposchkin, D. P., & Farber, H. W. (2002). Increasing plasmalogen levels protects human endothelial cells during hypoxia. *American Journal of Physiology Heart and Circulatory Physiology*, 283(2), H671–H679.